Continental Shelf Research 153 (2018) 64–74

Contents lists available at ScienceDirect

Continental Shelf Research

journal homepage: www.elsevier.com/locate/csr

Geochemistry and magnetic sediment distribution at the western boundary upwelling system of southwest Atlantic

Anna P.S. Cruz[a], Catia F. Barbosa[a,*], Arthur Ayres-Neto[b], Pablo Munayco[c], Rosa B. Scorzelli[c], Nívea Santos Amorim[a], Ana L.S. Albuquerque[a], José C.S. Seoane[d]

[a] Programa de Pós-Graduação em Geoquímica, Departamento de Geoquímica, Universidade Federal Fluminense, Niterói, Brazil
[b] Programa de Pós-Graduação em Dinâmica dos Oceanos e da Terra, Departamento de Geologia e Geofísica, Universidade Federal Fluminense, Niterói, Brazil
[c] Centro Brasileiro de Pesquisas Físicas, Rio de Janeiro, Brazil
[d] Programa de Pós-Graduação em Geologia, Departamento de Geologia, Universidade Federal do Rio de Janeiro, Rio de Janeiro, Brazil

ARTICLE INFO

Keywords:
Heavy minerals
Organic carbon
Upwelling
Mössbauer spectroscopy
Hydrodynamics
Sediment

ABSTRACT

In order to investigate the chemical and magnetic characteristics of sediments of the western boundary upwelling system of Southwest Atlantic we analyzed magnetic susceptibility, grain size distribution, total organic carbon, heavy mineral abundance, Fe associated with Mössbauer spectra, and Fe and Mn of pore water to evaluate the deposition patterns of sediments. Four box-cores were collected along a cross-shelf transect. Brazil Current and coastal plume exert a primary control at the inner and outer shelf cores, which exhibited similar depositional patterns characterized by a high abundance of heavy minerals (mean 0.21% and 0.08%, respectively) and very fine sand, whereas middle shelf cores presented low abundances of heavy minerals (mean 0.03%) and medium silt. The inner shelf was dominated by sub-angular grains, while in middle and outer shelf cores well-rounded grains were found. The increasing Fe^{3+}:Fe^{2+} ratio from the inner to the outer shelf reflects farther distance to the sediment source. The outer shelf presented well-rounded minerals, indicating abrasive processes as a result of transport by the Brazil Current from the source areas. In the middle shelf, cold-water intrusion of the South Atlantic Central Water contributes to the primary productivity, resulting in higher deposition of fine sediment and organic carbon accumulation. The high input of organic carbon and the decreased grain size are indicative of changes in the hydrodynamics and primary productivity fueled by the western boundary upwelling system, which promotes loss of magnetization due to the induction of diagenesis of iron oxide minerals.

1. Introduction

The dynamics of water masses and vortices along the continental shelf of southeastern Brazil determine primary productivity and sediment redistribution, leading to differences in sedimentation rates and downcore sedimentary profiles (Mahiques et al., 2010). Terrestrial runoff and aeolian transport also exert a considerable influence on particle deposition in the ocean, significantly influencing sediment composition.

Sediment transported along the continental shelf due to longshore currents, is deposited on preferential sites. The shape, size, and density of particles are determined by the residence time in the water column and by the types of fluid flow (e.g. laminar or turbulent flow) (Muehe and Carvalho, 1993). Accordingly, silt and clay are transported in suspension and are redistributed away from the coast by regional-scale currents.

Marine sediments act as good environmental records of land-sea interfaces. Such sediments have also been used to identify source areas and transport pathways of terrigenous matter, weathering, erosional processes, and climate change (Fagel, 2007). Sediment characteristics, such as concentration of magnetic minerals, mineralogy, grain size and magnetic susceptibility, are proxies of paleoenvironmental properties (Yamazaki et al., 2000). Furthermore, geochemical investigation of marine sediments can assess dissolution and precipitation of iron-bearing minerals at the oxic-anoxic boundary (Karlin and Levi, 1983), providing additional information about depositional and diagenetic processes, which affect the mineral composition of the sediments.

The magnetic properties of marine sediments are particularly sensitive to physical and chemical changes of the sedimentary environment (Pattan et al., 2008). Magnetic properties are mostly determined by the abundance of iron-rich minerals present in the sedimentary record (Chan et al., 1998; Villasante-Marcos et al., 2009). The oxidation state

* Correspondence author.
E-mail address: catiafb@id.uff.br (C.F. Barbosa).

https://doi.org/10.1016/j.csr.2017.12.011
Received 10 April 2017; Received in revised form 21 December 2017; Accepted 21 December 2017
Available online 23 December 2017

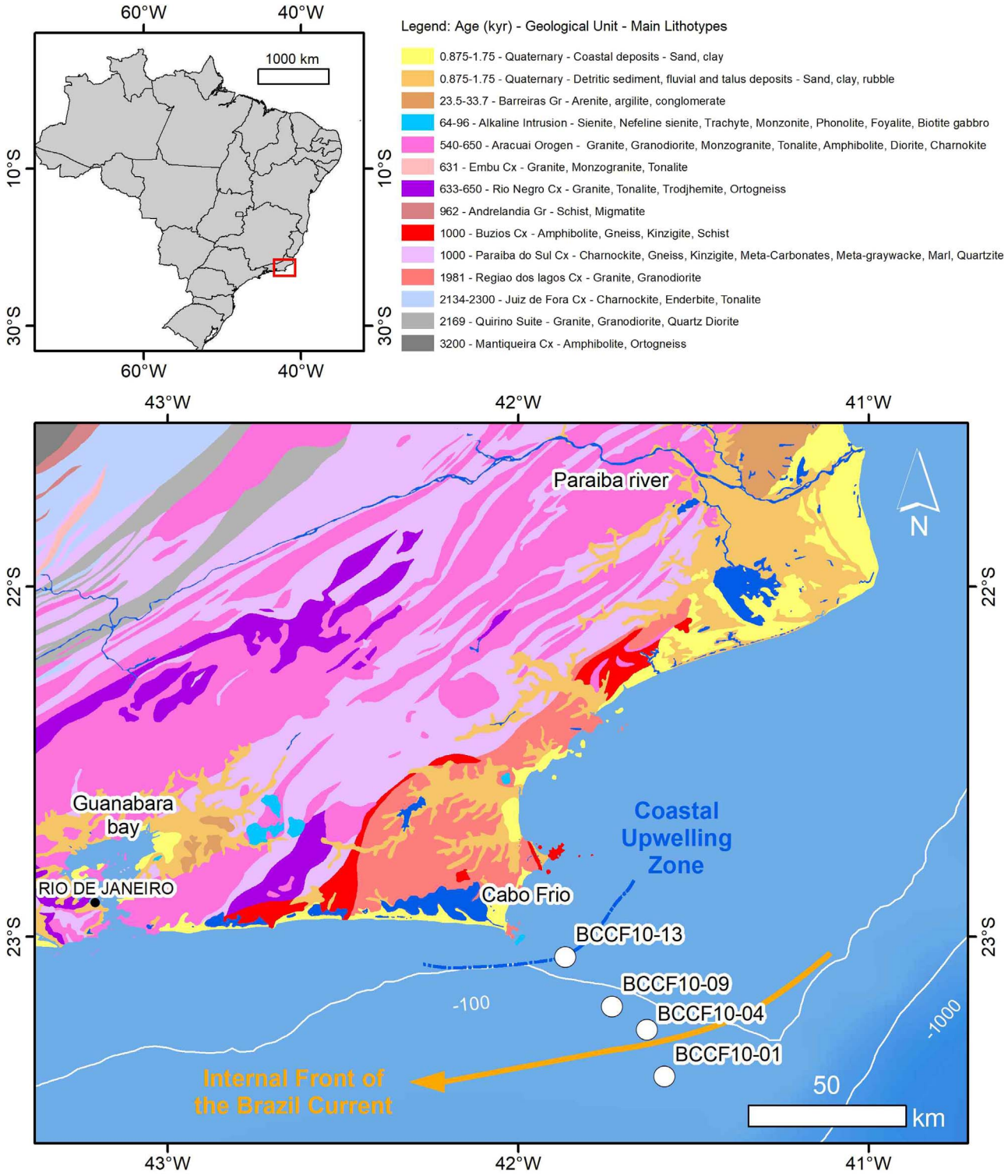

Fig. 1. Site of the cross-shelf transect with sampling stations at Brazil's Southeastern Continental Shelf. The geological map was modified from Geological Survey of Brazil (CPRM) (http://www.cprm.gov.br/en/Geology/Basic-Geology-4172.html - accessed on 30th, March 2017).

(Fe^{2+} or Fe^{3+}) revealed through Mössbauer spectroscopy (Hawthorne, 1988), can reflect oceanographic processes in the sediment through time (Frederichs et al., 1999). Mössbauer spectroscopy exploits the fact that changes in redox boundaries are consistent with environmental conditions (Drodt et al., 1997), which also allows identification of the sediment sources (Minai et al., 1981) and determination of the terrigenous input (Villasante-Marcos et al., 2009).

Here, we investigate the distribution of geochemical and magnetic properties of sediments in a cross-shelf transect to evaluate the role of current hydrodynamics in the sedimentation pattern of a western boundary upwelling system of Southeast Brazil.

2. Study Site

The southeastern Brazilian margin presents a complex hydrodynamic system, arising from a combination of physiographic features

of the shelf and the intense and persistent NE winds, currents and eddies that occur in this region (Calado et al., 2008). The hydrodynamic regime of this area is controlled by the Brazil Current (BC), which is a western boundary current off the South American continent that flows southward to the region of the Subtropical Convergence zone (Fig. 1). NE winds force the shoaling of South Atlantic Central Water (SACW) and the establishment of upwelling conditions. As a result, the dynamics of BC change, with a displacement of the internal front of this current away from the coast (Coelho-Souza et al., 2012; Mahiques et al., 2007).

Bathymetry also influences oceanographic dynamics modifying the energy and activity of mesoscale eddies (Calado et al., 2010). The presence of eddies is due to changes in coastline orientation in southeast Brazilian margin (from NE-SW to E-W) and the bathymetry gradient (Mascarenhas et al., 1971) that cause instabilities in the internal front of the BC. The BC flowing along the shelf break partially changes its direction to perpendicularly offshore causing cold-water intrusions of the SACW onto the shelf (Campos et al., 2000). The SACW creates baroclinic instability when it reaches the warm waters of the BC (Matano et al., 2010), forming eddies due to the shearing of distinct water masses. Thus, the upwelling system changes local oceanography and biological production (Belem et al., 2013), bringing cold, nutrient-rich waters to the surface and increasing biological productivity in the photic zone (Silveira et al., 2008). Most of the sediment transport patterns to the inner shelf are controlled by wind-driven circulation (NE winds) whereas, for the outer shelf, sediment deposition is influenced by the meandering motion of the BC (Mahiques et al., 2002). Mid-shelf deposition is controlled by mid-shelf wind curl that intensifies the upwelling and allows intrusion of nutrient-rich waters to the surface (Albuquerque et al., 2016; Belem et al., 2013).

The biological productivity in this shelf area is also affected by terrestrial influences, mostly via river input (Knoppers and Moreira, 1990; Mendoza et al., 2014) or aeolian dust (Rocha et al., 1975), which together introduce organic matter and essential nutrients (e.g. iron) into the seawater. Over the southeastern Brazilian shelf, the Paraíba do Sul River (located about 180 km north of Cabo Frio) has a considerable contribution of terrestrial sediments to the ocean margin, which can be entrained into the BC exerting significant influence on particle transport.

3. Material and methods

Sediments were collected using a box-core between April 24 and May 3, 2010, on board of the vessel Av. Pq. Oc. Diadorim of the Instituto de Estudos do Mar Almirante Paulo Moreira – IEAPM/Brazilian Navy. The cores were retrieved from four stations distributed in a cross-shelf transect across the southeastern Brazilian margin at water depths between 80 and 140 m. These cores were identified from outer to inner shelf: outer shelf core BCCF10-01 (23°24'S-41°35'W, 15 cm length); middle shelf cores BCCF10-04 (23°16'S-41°38'W, 22 cm length) and BCCF10-09 (23°12'S-41°44'W, 21 cm length); and inner shelf core BCCF10-13 (23°035'S-41°52'W, 11 cm length) (Fig. 1).

To analyze the magnetic susceptibility of the sediments, the cores were examined with a Multi-Sensor Core Logger (MSCL) manufactured by GEOTEK (Schultheiss and Weaver, 1992), which logs physical properties in sediment cores at small sampling intervals. The sampling resolution for these analyses was 0.5 cm.

Pore-water was extracted by using the Rhizon sampling technique (Seeberg-Elverfeldt et al., 2005) on cores BCCF10-01, −09 and −15 (representing outer, middle and inner shelf cores, respectively). Core BCCF10-15 was recovered from the same station as BCCF10-13 and was 21 cm in length. In order to analyze the diagenetic profile, eight samples were collected at the inner shelf and sampled at 2, 4, 5, 7, 9, 11, 16 and 21 cm of depth. Nine samples were collected at the middle and outer shelf cores between 1 and 16 cm, in which the upper 5 cm were analyzed with a 1 cm resolution, between 5 cm and 11 cm with a 2 cm resolution and below 11 cm with a 5 cm resolution. Pore-water was processed within an O_2-free glove bag, under N_2 atmosphere. The extraction of metal (Mn and Fe) in the samples was performed in a Chelex100 resin column. The concentrations of Mn and Fe were determined by Mass Spectrometry with an Inductively-coupled Plasma Source (ICP-MS; Thermo Fisher Scientific XSERIES 2), equipped with a conical mist chamber and a concentric nebulizer.

Sediment cores were sliced into segments of 1 cm thickness by extrusion and then stored at +4 °C. In the laboratory, each sample was further divided into subsamples and decarbonated using HCl (1 N) prior to determination of grain size, total organic carbon, and heavy minerals. Hydrogen peroxide was also added to remove the organic matter for grain size analyzes.

Grain-size measurements were performed every centimeter using a laser particle analyzer (CILAS 1064), which has a detection range of 0.02–2000 μm, using the grain size statistics method of Folk and Ward (1957) performed in GRADISTAT software version 8.0 (Blott and Pye, 2001).

Sediments undergoing assessment for Total Organic Carbon (TOC) were dried at 40 °C for 48 h and then approximately 0.01 g of each sample was crushed and packed in tin capsules to be analyzed in an automatic CHNS LECO analyzer coupled with a mass spectrometer. Results are expressed as dry weight percentages (%).

Approximately 15 g of each sample was dried at 50 °C and crushed for separation of heavy minerals. A 5 g aliquote was separated with bromoform (density 2.89 g/cm^3). Less dense minerals floated on the bromoform, whereas heavy minerals settled. The floating material was discarded, and the settled minerals were filtered, washed with acetone and distilled water, and dried for subsequent weighing. The abundance of heavy minerals was calculated as the final weight/initial weight with values given as percentages (%). After separation, heavy minerals were identified using a Scanning Electron Microscope equipped with an Energy Dispersive Spectrometer (SEM-EDS; Philips XL 30). Seventy-two samples were analyzed using SEM, and EDS was performed in 100 heavy mineral grains in each core. The heavy minerals were analyzed to obtain the shape and surface characteristics of the grains using the software IMAQ Vision Builder with magnification of 200× from the SEM images. The elementary composition provided by EDS enabled the identification of the minerals according to Dana (1984).

The roundness degree evaluation was applied only to heavy minerals and not to the fraction (dominated by quartz) floated on bromoform. The roundness of the heavy minerals was calculated from the 2D images according to Cox (1927) following the Eq. (1):

$$R = 4\pi A/P^2 \quad (1)$$

where A is the particle area and P is the particle perimeter. The roundness limits are expressed according to Powers (1953) (Table 1).

To determine the Fe^{3+}:Fe^{2+} ratio, samples were dried at 40 °C and crushed. Approximately 1 g of each sample was packed into capsules and sent to the Brazilian Center of Physical Research for Mössbauer spectroscopy analysis. The ^{57}Fe Mössbauer spectroscopy in transmission geometry was performed at room temperature (RT) in a 512-channel Halder spectrometer. The drive velocity was calibrated using a ^{57}Co source in Rh matrix and an iron foil, both at RT. The measurements were performed at low and high velocity, with an average recording

Table 1
Classes of the adopted scale of roundness.

Grade Term	Class limits
Very angular	0.12–0.17
Angular	0.17–0.25
Subangular	0.25–0.35
Subrounded	0.35–0.49
Rounded	0.49–0.70
Well rounded	0.70–1.00

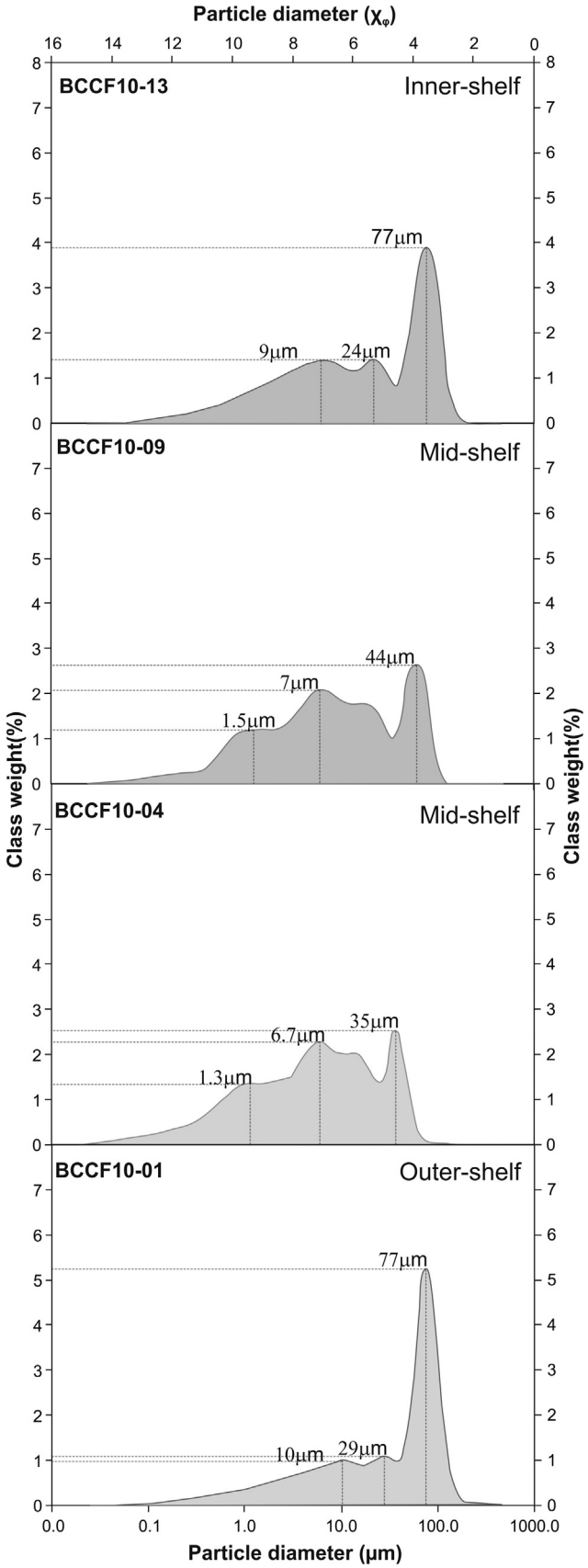

Fig. 2. Mean grain-size distributions of sediments from inner-shelf (BCCF10-13; n = 11 (a)), mid-shelf (BCCF10-09, n = 21 (b), BCCF10-04, n = 22 (c)) and outer-shelf (BCCF10-01, n = 15 (d)) cores.

time of 24 h per sample. The Mössbauer absorbers were prepared with 20 mg/cm^2 of the sample. NORMOS code was used for the spectrum analysis based on least-squares fitting routine, assuming each spectrum to be a sum of Lorentzian lines grouped into quadrupole doublets and magnetic sextets. Isomer shifts are reported in relation to α-Fe. The Fe^{3+}:Fe^{2+} ratio was calculated from the relative areas of doublets associated with Fe^{3+} and Fe^{2+}, respectively.

The chronology and the sedimentation rates were determined from the ^{210}Pb activity based on decay of the ^{238}U series following the method described by Moore (1984) as reported by Sanders et al. (2014). The sedimentation rate was calculated by the decay curve in relation to depth, providing an age-depth model for the last 150 years.

4. Results

All cores were characterized by tri-modal grain-size distributions (Fig. 2). The inner (BCCF10-13) and outer (BCCF10-01) shelf cores presented similar grain-size distribution patterns, exhibiting peaks at approximately 9–10 μm (frequencies between 1.0% and 1.3% weight), 24–29 μm (frequencies between 1.1% and 1.3% weight) and 77 μm (frequencies between 3.9 to 5.2% weight), indicating that more than 60% of these cores were composed by very fine sand (63–125 μm) and coarse silt (31–63 μm). Middle shelf cores (BCCF10-09 and 04) were similar to each other, with grain sizes peaking at 6.7–7 μm (frequencies between 2.1% and 2.2% weight) and at 35–44 μm (frequencies between 2.5% and 2.6% weight), and exhibiting two plateaus from ~1.0 to ~2.3 μm (frequencies between 1.1% and 1.3% weight), and from ~10 to ~19 μm (frequencies between 1.8% and 2.0% weight), revealing a mixture of coarse to medium silt (8–31 μm) throughout the cores (Figs. 2 and 3).

Heavy minerals such as monazite, pyrite, rutile, sillimanite, titanite, zircon, ilmenite, hornblende and hematite were found in all cores (Fig. 4). Heavy mineral abundances in the inner (BCCF10-13) and outer (BCCF10-01) shelf cores reach higher values than the middle shelf cores (BCCF10-09 and −04) (Fig. 3b). For the inner and outer shelf cores, heavy mineral abundance ranged from 0.09% to 0.4% and from 0.03% to 0.13% respectively, whereas for the two mid-shelf cores it ranged from 0% to 0.03% (BCCF10-09) and 0.008–0.07% (BCCF 10-04) (Fig. 3b).

The surface texture of the heavy minerals is characterized by the predominance of well-rounded grains with a size variation of approximately 63–200 μm for the middle and outer shelf cores. The roundness of the particles in the outer shelf core (BCCF10-01) ranged from 0.64 to 0.98 (mean 0.88) whereas, for the middle shelf cores (BCCF10-09 and −04), roundness of the heavy minerals ranged from 0.62 to 0.96 (mean 0.84) and 0.47–0.98 (mean 0.84) respectively, all representing sub-rounded to well-rounded particles (Table 1). A larger roundness variation interval (between 0.15 and 0.76: sub-angular to well-rounded), with dominance of sub-angular shapes, and a lower mean roundness were observed in the inner shelf core (BCCF10-13) (Figs. 3c and 5a).

Lower values of organic carbon were observed for the inner and outer shelf cores compared to middle shelf cores. Organic carbon (TOC) content varied between 0.7% and 1.3% for the inner shelf core and between 0.6% and 1.7% for the outer shelf core (Fig. 3d). The middle shelf cores (BCCF10-09 and 04) presented organic carbon contents ranging from 0.8% to 2.3% and from 1.5% to 2.1%, respectively.

Positive MS values were found for the inner (BCCF10-13) and outer (BCCF10-01) shelf cores (Fig. 3e). The inner shelf core presented values ranging from 13 to 15 $\times 10^{-6}$ SI and the outer shelf core presented values ranging from 14 to 20 $\times 10^{-6}$ SI, with values increasing from the bottom of the cores to a depth of 4 cm before decreasing thereafter to the top of the cores (Figs. 3e and 6a, d). These cores displayed higher MS values compared with middle shelf cores, which predominantly showed negative MS values ranging from −17 to −3 $\times 10^{-6}$ SI and from −7 to 3 $\times 10^{-6}$ SI (for BCCF10-09 and −04 respectively), with values increasing towards the top of cores (Figs. 3e and 6b, c).

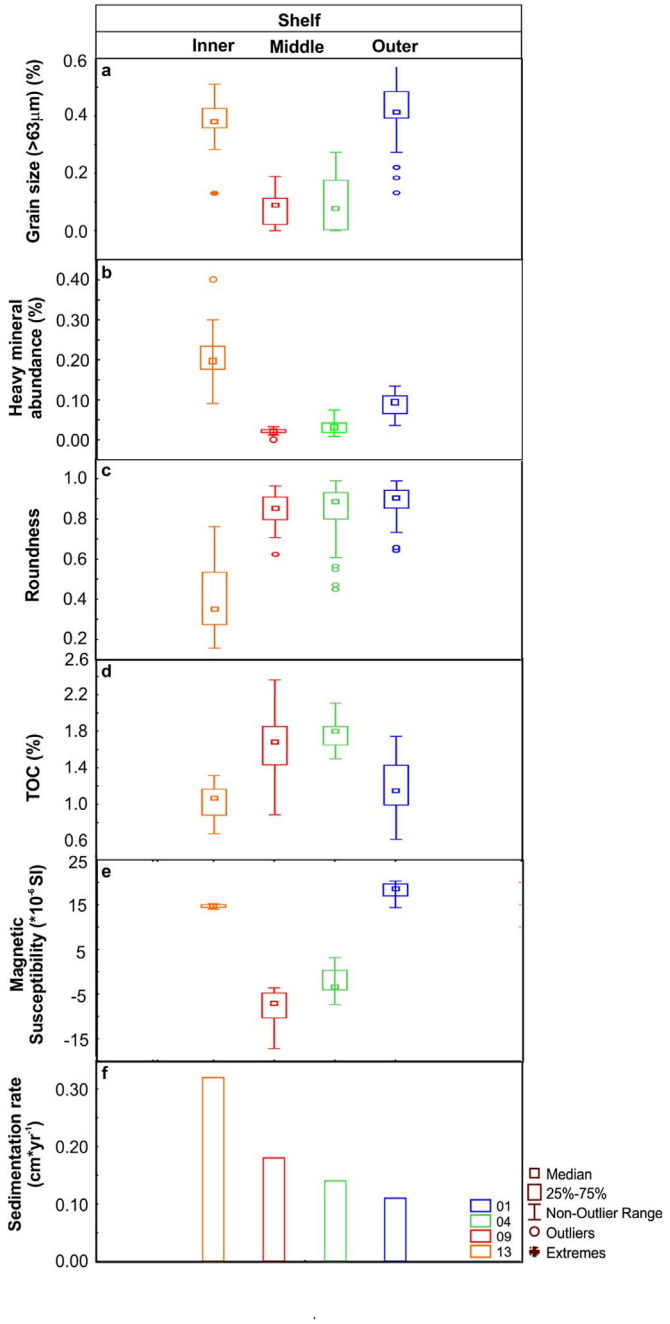

Fig. 3. Box-plots of core variables: (a) grain size distribution (> 63 μm), (b) heavy mineral concentrations (> 63 μm), (c) heavy mineral roundness, (d) TOC, (e) magnetic susceptibility and (f) bar plot of sedimentation rate (Sanders et al., 2014) for the inner cores BCCF10-13 (yellow), middle cores BCCF10-09 (red) and, BCCF10-04 (green) and outer core BCCF10-01 (blue).

The Fe^{3+}:Fe^{2+} ratio for the inner shelf core showed lower values 0.5–0.65), showing the dominance of Fe^{2+} near the coast, when compared with the higher values of the middle and outer shelf cores 5–7). Fe^{3+}:Fe^{2+} ratio increased from the bottom of the core to the top, except in the inner core, where the ratio is highest at the base of the core. For the outer shelf core, the Fe^{3+}:Fe^{2+} ratio ranged from 5.5 to 7 and Fe^{3+} was dominant (Fig. 6d). The proportion of Fe^{3+} increased towards the top of the core, matching the increasing MS values. For middle shelf core BCCF10-09 the Fe^{3+}:Fe^{2+} ratio ranged from 6.16 and 6.34 and the proportion of Fe^{3+} increased towards the top of the core, as for MS values. For middle shelf core BCCF10-04, in which MS values were negative from the bottom of the core up to a depth of 5 cm and were positive from 5 cm depth to the top of the core, mineral proportions increased from the base to the top of the core, with the Fe^{3+}:Fe^{2+} ratio ranging between 6 and 7 (Fig. 6b, c).

We measured Mn and Fe in the pore water of the inner (BCCF10-15), mid (BCCF10-09) and outer (BCCF10-01) shelf cores (Fig. 7). For the inner shelf core, Mn and Fe concentrations decreased between 0 and 5 cm core depth, ranging from 12 to 5 μM and 230 to 50 μM, respectively. Thereafter, between 5 and 10 cm depth, Mn and Fe concentrations increased 5–8 μM and 50–100 μM, respectively), with subsequent small reductions in concentrations towards the bottom of the core. For the middle shelf core BCCF10-09, Mn and Fe concentrations both increased with depth between 2 and 4 cm, ranging from 1.2 to 7 μM and 40–77 μM, respectively, and then decreased with depth towards the bottom of the core, ranging from 7 to 0.9 μM and 55 to 34 μM (Fig. 7b). In the outer shelf core, the Mn and Fe concentrations increased between 1 and 2 cm core depth, ranging from 1.7 to 4.1 μM and 20 and 80 μM (Fig. 7c). Mn and Fe values decreased for the outer shelf core for depths between 2 and 4 cm, ranging from 4 to 2.9 μM and 20–80 μM, respectively. Deeper than 4 cm, the concentration of Mn decreased and the Fe concentration increased gradually with depth, ranging from 2.7 to 4 μM and 19–120 μM, respectively.

5. Discussion

5.1. Sediment deposition and accumulation processes across the SE Brazilian continental shelf

In the cross-shelf transect of southeastern Brazilian margin, the depositional process was similar between inner and outer shelf, but differed from the mid-shelf. Sand predominated in inner and outer shelf cores (i.e. greater abundance of coarse grains (> 63 μm) and heavy minerals) (Fig. 3a and b), whereas mud with colloidal organic matter deposition (i.e. high organic content and fine sediments) dominated mid-shelf cores. Differences in the poly-modal grain-size distributions amongst cores suggest that sediments were transported and deposited by different processes. As shown in Fig. 2, central shelf cores present two peaks and two plateaus in their grain-size distribution patterns, whereas inner and outer shelf cores presented a tri-modal grain-size distribution. A broader distribution of the grain size modes were evident for the middle shelf cores (BCCF10-09 and −04) compared with the coarse sediments (> 31 μm) of inner and outer shelf cores (BCCF10-13 and −01). The dominance of fine sand and coarse silt fractions in inner (BCCF10-13) and outer (BCCF10-01) shelf cores is associated with changes of provenance and higher energy transport than the middle shelf cores. Sediment dispersion over the shelf is linked to fluvial plumes and the BC, which influences the inner and outer shelf cores. Sediment accumulation in the inner (BCCF10-13) shelf core indicates the influence of the coastal plume that promotes sediment transport primarily to regions near the coast, which presents the highest sedimentation rate (0.32 cm/year) (Fig. 3f) (Sanders et al., 2014). Most of the Paraíba do Sul river discharged suspended sediment is subsequently transported southward (Gyllencreutz et al., 2010) by the internal front of the Brazil Current, accumulating on the outer shelf. According to Wanderley et al. (2013), the sedimentation rate at the Paraíba do Sul River mouth has varied over recent decades, presenting a low sedimentation rate before 1950 (0.05–0.1 g cm^2.yr) and a significant increase thereafter to around 0.5–0.7 g cm^2.yr. In addition, that study also demonstrated increased sedimentation rates from north to south, with sediments carried by BC. Thus, the southward dispersion of sediments coming from the Paraíba do Sul River may explain the accumulation patterns found in the outer shelf of southeastern Brazilian margin.

The northern portion of southeast Brazilian coast presents Pre-Cambrian rocks that are considered as the primary source of heavy mineral deposits in the region (Anjos et al., 2007). A secondary source of these minerals could be associated with sedimentary deposits of the

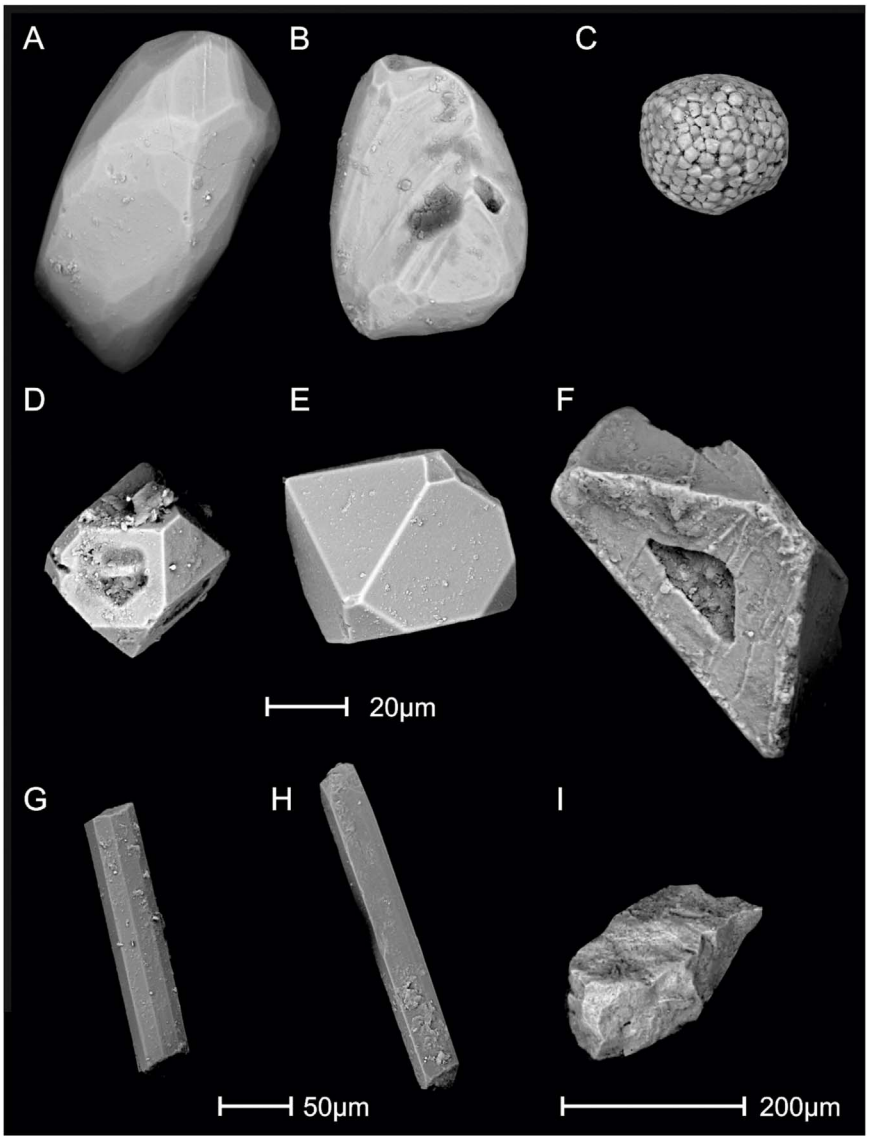

Fig. 4. Scanning electron microscopy images of heavy minerals found in the study area: (a) zircon, (b) monazite, (c) pyrite, (d) rutile, (e, f) ilmenite, (g) hornblende, (h) sillimanite, (i) hematite.

Miocene Barreiras Formation (Rossetti et al., 2011), from which minerals could be eroded and transported to the southeastern Brazilian shelf via the coastal drainage system (Suguio, 1980). The heavy mineral assemblages found in the cross-shelf transect indicate a provenance from igneous and metamorphic rocks derived from siliciclastic metasediments (Remus et al., 2008), with a predominance of granitoids and in minor amount of mafic and alkaline rocks from Cabo Frio Domain and adjacent areas.

A high abundance of heavy minerals (> 0.08%) and large grain size (> 63 μm) was observed in the outer (BCCF10-01) and inner (BCCF10-13) shelf cores (Fig. 3b), but the inner shelf core presented the highest abundance due to its proximity to the coastal area as well as by winnowing process (reworking by high velocity currents). The abundance of heavy minerals co-varies with increasing grain size (up to 63 μm) and greater input of terrestrial sediments on the outer (BCCF10-01) and inner (BCCF10-13) shelf cores compared to the middle shelf cores (BCCF10-04 and −09) that had lower heavy mineral abundances (Fig. 3b) and higher percentages of silt and clay (Fig. 3a). Higher organic content in the middle shelf cores, (Fig. 3d) and the $\delta^{13}C$ from organic matter (−21‰), as in Sanders et al. (2014) indicate a marine origin for the organic matter and dominating authigenic condition. The average TOC content, in the middle shelf, produced by biogenic processes, was ~2% and can be associated with the predominance of fine grains (< 63 μm) under upwelling influence, which promotes higher productivity compared to inner (BCCF10-13; 1.39%) and outer (BCCF10-01; 1.21%) shelf cores (Fig. 3d).

Sediment transport can modify grain size through abrasive processes and, mainly, hydraulic sorting (Chorley et al., 1985). Minerals such as zircon, monazite and rutile, amongst other ultra-stable minerals found (Fig. 4), are able to withstand multiple cycles of sediment reworking due to their high stability under weathering and diagenetic processes, which allows them to remain throughout the depositional record (Morton and Hallsworth, 1999). Minerals become more rounded during the transport process, which reduces the original faces on grains by abrasion. We observed this pattern in our cores recovered from middle and outer shelf (Figs. 3c, 5).

The dominance of rounded and well-rounded heavy mineral grains was found in the middle (BCCF10-09 and −04) and outer (BCCF10-01) shelf cores (with mean values of 0.84, 0.84 and 0.88, respectively) suggesting highly reworked material and long-distance transport (Fig. 5b, c, d), which reduced the crystal faces due to abrasive processes. According to Rocha et al. (1975), the degree of roundness of the sand fraction (125–250 μm) increases in the southernmost region of Cabo Frio continental shelf, where these authors found sub-angular to sub-rounded grains. They also demonstrated that the abundance of heavy minerals (with densities above 2.87) was less than 0.5% of the

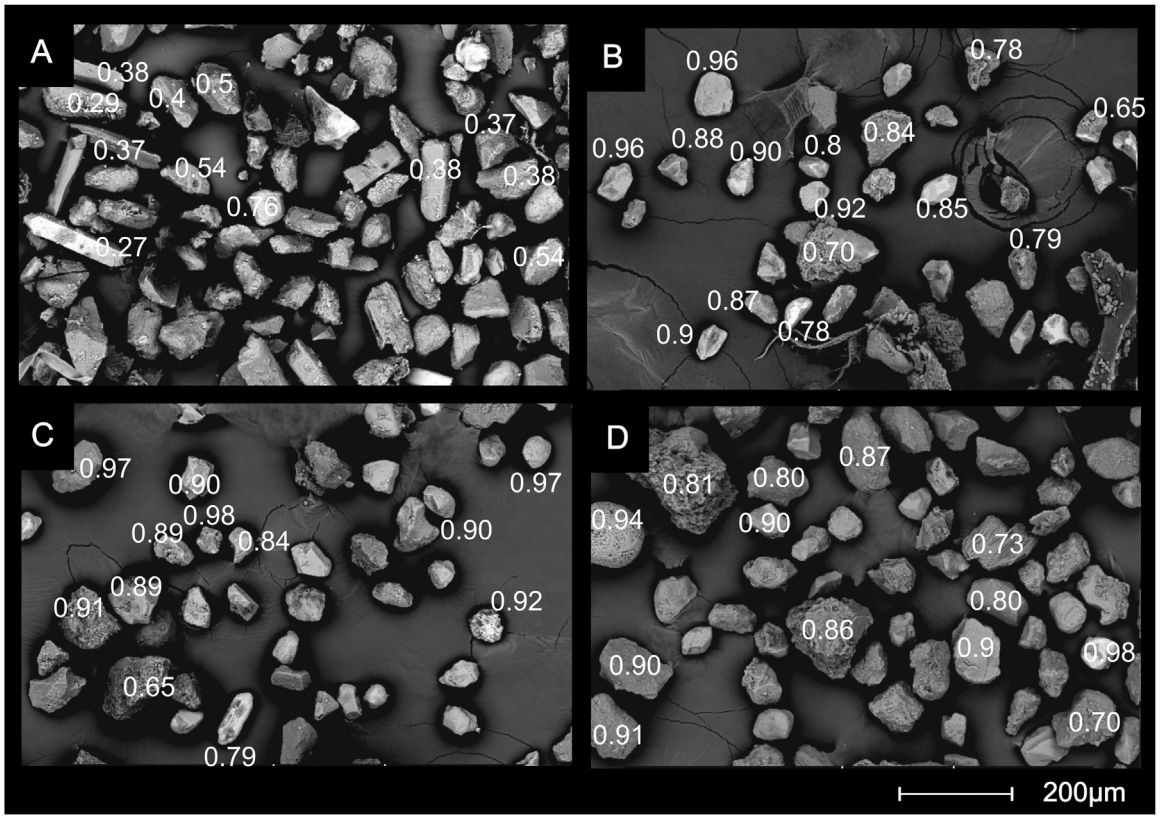

Fig. 5. Size and shape of heavy minerals found in the inner shelf core BCCF10-13 (A), mid-shelf cores BCCF10-09 (B) and BCCF10-04 (C), and outer shelf core BCCF10-01 (D). The number (white) represents the roundness of the grains.

sand fraction and that they were higher in the north of Cabo Frio shelf because of the influence of rivers.

Rounded zircon grains can indicate the source area as being sedimentary (Nobrega et al., 2008) or parametamorphic rocks. Presence of unstable minerals such as hornblende (with densities of 3.0–3.4) can also reflect proximity to the source area. The inner shelf core (BCCF10-13) presented more angular minerals of large grain size (> 63 µm) and unstable minerals compared to the middle and outer shelf cores, indicative of proximity to mineral source areas, which can be potentially linked to coastal plumes carrying detritic material to the inner shelf. Deposition of well-rounded grains coarser than 63 µm in the outer shelf core may have occurred because of displacement of the BC from the coast. After the South Equatorial Current bifurcates into the BC (off the South American coast at 10° − 14°S), the BC moves southward along the coast (Rodrigues et al., 2007). However, the change in shoreline orientation (from N-S to E-W) that occurs in southeast Brazil promotes a displacement of the BC from the coast, thereby increasing particle transport to the outer shelf. Therefore, the BC acts transporting the grains to long distances away from the coast promoting higher abrasion and roundness of sediment particles.

According to Viana et al. (1998), sediments derived from the discharge of the Paraiba do Sul River are deposited in areas adjacent to the Buzios and Cabo Frio region, 150 km south of the river mouth. Paraíba do Sul plumes during higher freshwater discharge (760 m^3/s) tend to disperse parallel to the coast southwards from the river mouth (de Oliveira et al., 2012), enhancing sediment dispersion to the shore by BC transport.

On the outer shelf, the intense action of the internal front of the BC

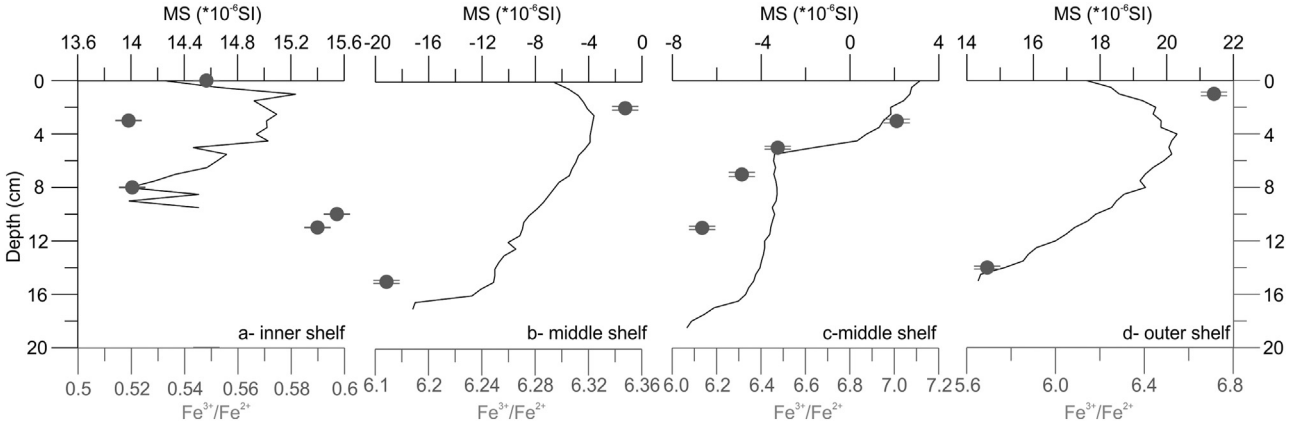

Fig. 6. Plots of variations in magnetic susceptibility (x10^{-6} SI) (black line) and Fe^{3+}:Fe^{2+} ratios (green) versus depth (cm) for the inner core BCCF10-13 (a), middle cores BCCF10-09 (b) and BCCF10-04 (c) and outer core BCCF10-01 (d).

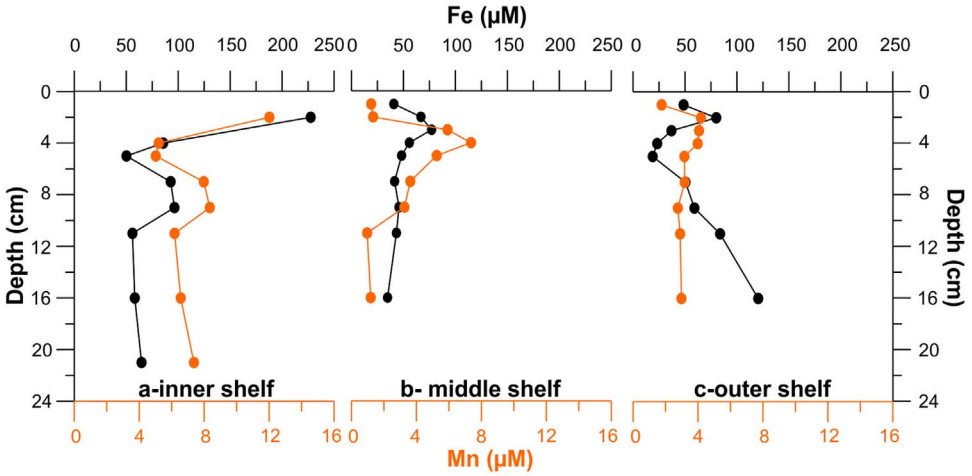

Fig. 7. Elemental concentration of Fe (black line) and Mn (yellow line) for the inner core BCCF10-15 (a), middle core BCCF10-09 (b) and outer core BCCF10-01 (c).

promotes an increase on the grain size (medium to coarse) with sands between moderately to well-rounded, dominated by siliciclastic and carbonatic sediments (Viana et al., 1998), and prevents the deposition of mud and organic material (Mahiques et al., 2010, 2004). The influence of the BC in the sedimentation process in outer shelf areas is also reported at São Paulo Bight and São Sebastião Island (Mahiques et al., 2002), where the BC meanders enhance the suspended sediment transport towards outer shelf regions.

Thus, oceanographic dynamics greatly impact sediment deposition and accumulation in the southeastern Brazilian margin. Sediment distributions reveal differences in depositional processes across the shelf, which are summarized in the conceptual model presented in Fig. 8. In this model, the similarities are apparent between the inner and outer shelf cores, with their predominance of detritic material coming from the land being influenced, respectively, by coastal plumes and the BC. However, authigenic material influenced by SACW intrusions into the photic zone predominates in the mid-shelf cores, contributing to a higher deposition and accumulation of organic carbon and fine sediments in the central portion of the shelf.

5.2. Magnetic susceptibility reveal redox processes along the SE Brazilian

Magnetic susceptibility is related to the mineralogical sediment composition of the clastic and authigenic material. Minerals such as magnetite and other iron oxides have high MS, while carbonates, silica and organic content present diamagnetic properties that may reduce MS, often resulting in negative values (Evans and Heller, 2001). In median cross shelf distribution (Fig. 3e), the inner and outer shelf cores (BCCF10-13 and −01, respectively) displayed high MS values, unlike middle shelf cores (BCCF10-09 and 04). Lower MS values found for middle shelf cores were the result of the predominance of fine particles in both cores (Fig. 3a). Fine particles promote greater water absorption because of their ability to adsorb electrolytes and organic material, affecting the composition and degree of sediment consolidation (Busch and Keller, 1981; Cruz et al., 2013). Thus, the high water content of the middle shelf cores (BCCF10-09 and −04) (Cruz et al., 2013) is associated with the texture of its grains and the presence of organic matter (Fig. 3d), which reduces its MS values. However, in the vertical profile (Fig. 6), the water content and the MS values decrease with depth, which was not expected. This can be attributed to dissolving ferrimagnetic and/or paramagnetic minerals, therefore increasing the proportion of diamagnetic minerals, thus decreasing the MS. The reduced MS of core BCCF10-09 (Fig. 6b) could also be attributable to preferential dissolution of fine particles, by which Mn and Fe are actively liberated to the pore water due to reduction of Fe and Mn hydroxide in the sub-oxic zone (below 4 cm depth) (Fig. 7b) (Passier et al., 1998).

The diagenesis of iron does alter MS values of sediments. Oxidation of organic matter is the driving mechanism for early diagenetic

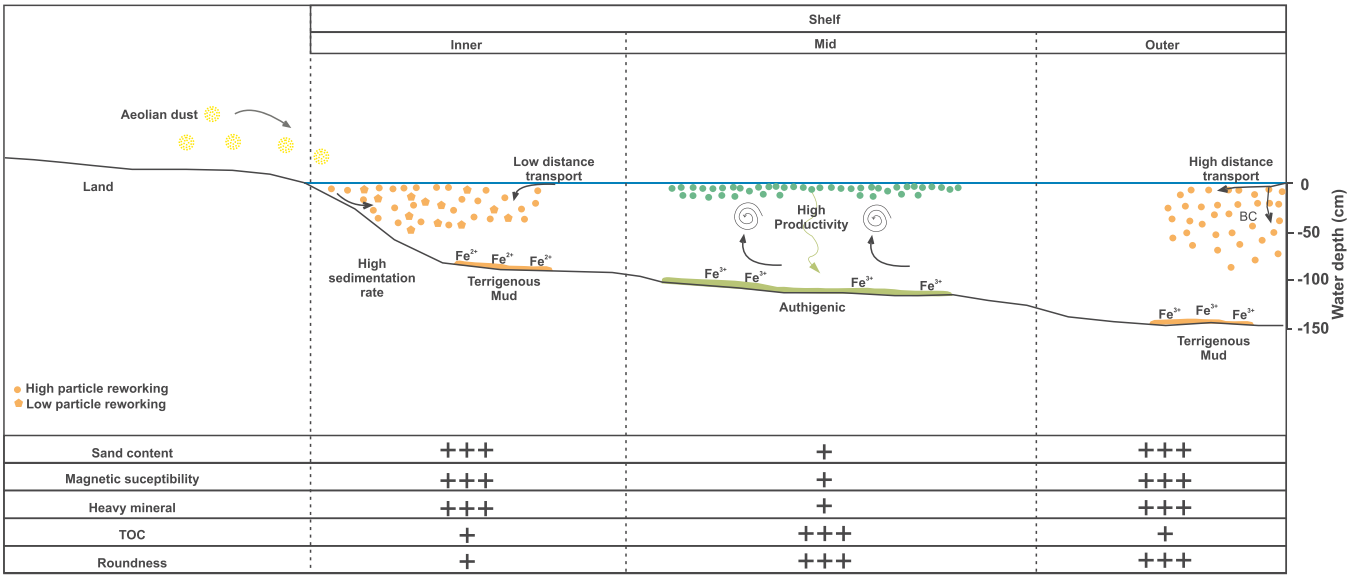

Fig. 8. Conceptual model of cross-shelf sedimentation and chemical distribution patterns of the Southeast Brazilian continental shelf.

reactions in sediments, promoting the oxygen consumption. At levels where oxygen is absent, decomposition of organic matter is driven by nitrate reduction and subsequently by reduction of the oxy-hydroxides of Fe and Mn, which releases Fe^{2+} and Mn^{2+} into the pore water (van Santvoort et al., 1997). After diffusion towards the top of the sediment, these ions re-precipitate as oxy-hydroxides when they encounter oxygenic conditions (Berner, 1984). In typical eastern boundary upwelling systems, such as that of Angola-Namibia, MS is dominated by paramagnetic and diamagnetic minerals. High loss of magnetization can occur because of the increased organic content in these high productivity areas (Yamazaki et al., 2000), developing reducing conditions in the sediment and the dissolution of Fe oxides and oxyhydroxides

The outer shelf cores (BCCF10-01) present high MS (Fig. 6a, d) as a result of increased percentages of coarse grains and high Fe^{3+}:Fe^{2+} ratio. This may indicate considerable terrestrial input due to the influences of the coastal plume and Brazil current. Fe in the coastal marine environment represents terrestrial inflow that is transported by wind and rivers (Bucciarelli et al., 2001). Both transport modes can occur on the southeastern Brazilian coastal margin, but the influence of rivers definitely exceeds the contribution of wind because the prevailing wind direction for most of the year is from northeast (Valentin, 2001), so that aeolian sediments are mainly deposited on the dune fields present on the continental margin.

High concentrations of Mn and Fe at 2 cm depth for the outer shelf core (BCCF10-01) (Fig. 7c) indicate the beginning of reducing conditions in the sediment, favoring diffusion of these elements (Schulz and Schulz, 1999). Magnetic intensities increased for core depths up to 5 cm, indicating low dissolution of Mn- and Fe-oxide minerals. However, the reduced MS at depths > 5 cm occurs at the same time as an increase in Fe^{2+} in sediments (reduced Fe^{3+}:Fe^{2+} ratio) (Fig. 6) and the iron concentration reduction in the pore water (Fig. 7). The decrease in concentration of Fe in the pore water may be associated with hydrodynamics and bioturbation that can intensify redox cycling. Bioturbation promotes oxygen entry into sediments and re-oxidation of free iron in pore water. Also, intrusion of oxygen-rich water, such as from the SACW, onto the continental shelf in long term states, might alter the redox conditions of the environment, contributing to re-oxidation processes, which contribute to oxidize Fe^{2+} to Fe^{3+}.

The ratio of Fe^{3+}:Fe^{2+} increased towards the top of cores BCCF10-01, −04 and −09 (Fig. 6), indicating predominance of Fe^{3+} at the top relative to the base of these cores. The decrease of Fe^{3+}:Fe^{2+} ratio at the base of these cores indicates that Fe^{3+} had been reduced to Fe^{2+}. In reducing environments, the reduced iron can interact with sulfate, via bacterial metabolic processes, forming iron monosulfide and later pyrite (Canfield, 1989). This Fe^{2+} may also be free in the pore water of the inner shelf core (BCCF10-15), which may diffuse to the deepest regions of the sediment (Scorzelli et al., 2008). In marine sediments, pyrite formation is controlled mainly by the amount and reactivity of organic matter buried in the sediment (Berner, 1984). However, in sediments of the southeastern Brazilian continental shelf, the iron does not act as a limiting factor, so that sulfur can eventually enter into the organic matrix to form pyrite (Diaz et al., 2012). The high Fe^{3+}:Fe^{2+} ratio found at the top of the outer shelf core (BCCF10-01) (Fig. 6d) could also be linked to the presence of heavy iron oxides, such as hematite (which we identified using SEM-EDS Fig. 4i).

In the middle shelf area, increased Fe^{3+}:Fe^{2+} ratio were associated with reduced grain size (Fig. 6b, c). The predominance of Fe^{3+}, mainly at the top of these cores, could be associated with the capacity of clays to adsorb and replace some elements (such as Al) in its structure (Stucki et al., 1984). The Fe^{3+} present in the form of iron hydroxide could precipitate onto and cover clays, as shown in Fig. 9.

According to Chen et al. (1996), the Fe^{3+}:Fe^{2+} ratio in marine sediments increases with increasing distance from coastal areas, which may explain the low ratio we found for the inner shelf core (BCCF10-13) (Fig. 6a). This core also presented lower clay content and coarse grains predominated. The high values of Fe^{2+} could also be connected to early diagenesis and the weathering of aluminosilicates, mirroring results found by Chen et al. (1996) and Schulz and Zabel (1999). This scenario arises because aluminosilicates are easily dissolved (less stable) during the transport process (i.e. runoff, river inflow and ocean currents).

Thus, two different depositional patterns are observed across the continental shelf at Cabo Frio, as previously shown by the basic controls on MS values, grain size, terrigenous sediment input and organic matter content (Fig. 8). The cores from the inner and outer shelf presented high MS values associated with an increase in grain size and a reduction of organic content. Despite finding a high abundance of heavy minerals in the inner shelf core, the Fe^{3+}:Fe^{2+} ratio was lower than that of the outer shelf. The increased sedimentary Fe^{2+} indicates that most of the iron came from aluminosilicates indicating proximity to the source area and evidencing transport by coastal plumes. For the outer shelf core, higher MS and large well-rounded particles (> 63 μm) associated with a high Fe^{3+}:Fe^{2+} ratio indicates predominance of iron oxy-hydroxides (paramagnetic and ferromagnetic minerals), which were carried to longer distances to the outer shelf by fluvial current (e.g. from Paraíba do Sul River) and by BC. For the mid-shelf cores, the dominance of organic material and fine particles resulted in low MS for this area. The high fine particle input (i.e. clay) can be associated with an increase in the Fe^{3+}:Fe^{2+} ratio in the sediment due to iron adsorption by the clay structure (Fig. 9). This higher accumulation of organic carbon and fine sediments (Fig. 3a,d) may have arisen from intrusions of the SACW, controlled by the mid-shelf wind curl that intensifies upwelling in the central portion of the shelf.

6. Conclusions

Sediment distributions revealed differences in depositional processes across the southeast Brazilian continental shelf. In the inner and outer shelf areas, detritic sediments coming from the land and transported by coastal plumes and currents predominated. The increased abundance of detritic sediments on the outer shelf is interpreted as arising from the change in shoreline orientation (NE-SW to E-W), which promotes a displacement of the BC from the coast and thereby enhances particle transport to the outer shelf. However, authigenic materials predominate in the central portion of the shelf, where the increase in the organic productivity, driven by cold-water intrusions of the SACW into the photic zone, contributes to deposition and accumulation of organic carbon and fine sediments.

These changes in the sediment distribution between inner-outer and middle shelf cores also resulted in MS alterations. MS in the middle shelf zone is controlled by diamagnetic minerals, such as carbonate and silica, with loss of magnetization in this zone due to increased organic content as a result of the intrusion of SACW increasing the productivity. In this region, Fe^{3+} could act on the replacement of some elements in the clay structure. In the outer shelf, given the contribution from BC in the transport particles to offshore, Fe^{3+} predominates because of the presence of iron-oxides, such as hematite.

In the inner shelf, sedimentary reworking induced by coastal plumes and upwelling dynamics causes re-suspension of deposited organic material in the oxic water column, which could lead to rapid degradation. In this case, high MS values are due to decreased organic content and may be closely linked to an increase of iron minerals in the environment. However, a predominance of fine sand in the inner shelf, promotes a decrease in the Fe^{3+}:Fe^{2+} ratio, which might also be connected to early diagenesis, reducing Fe^{3+} to Fe^{2+}, and releasing Fe^{2+} in pore water. Aluminosilicate weathering is shown by their distribution, as they are easily dissolved and therefore less stable during transport, and thus predominate close to the source area.

Thus, geochemistry and magnetic properties of sediments distinguished middle shelf from inner-outer shelf sites in a cross-shelf transect for the last 150 years.

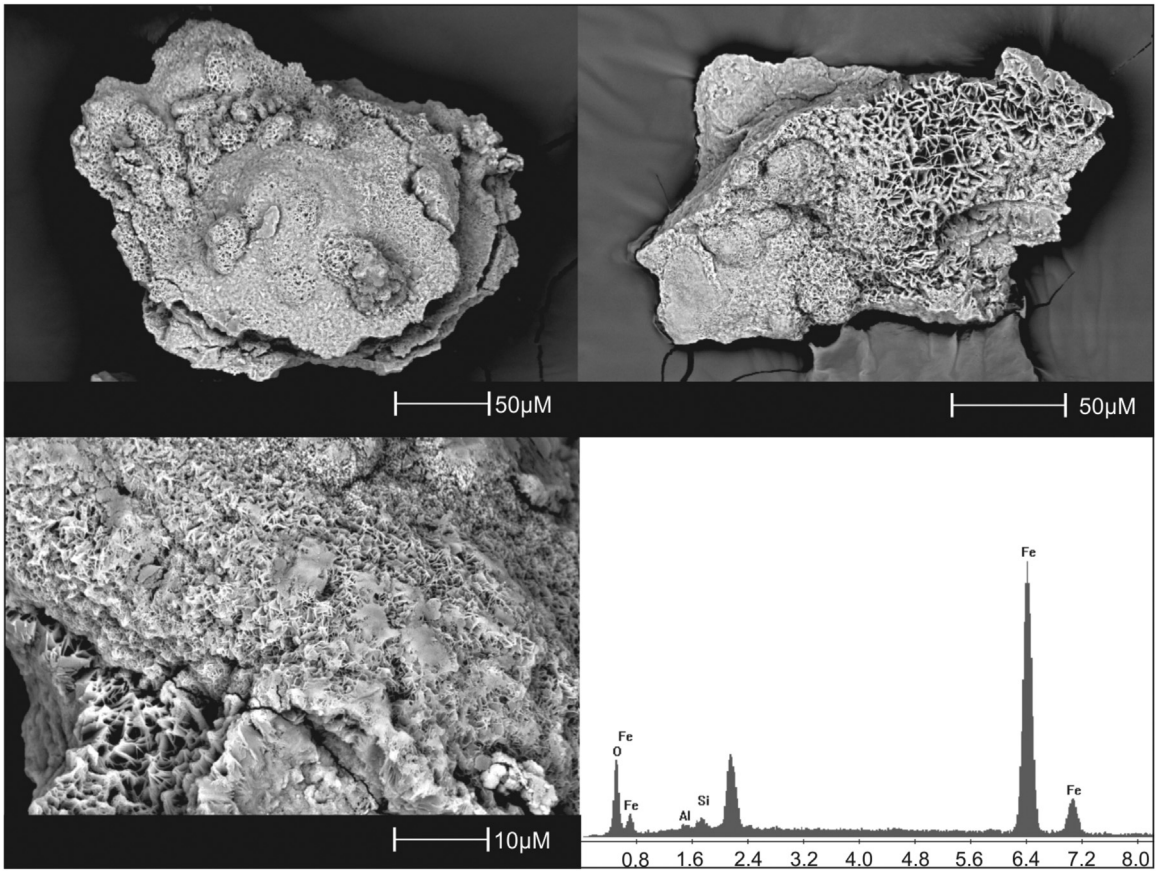

Fig. 9. Scanning electron microscopy images and energy dispersive spectroscopy (EDS) (SEM-EDS; Philips XL 30, with secondary electron imaging) showing iron nucleation coating in clays of middle core BCCF10-09.

Acknowledgements

We thank the upwelling project group (Petrobras Geochemistry Network and Ramses Capilla) and the crew of the Diadorim vessel for assistance with sampling. APSC thanks CNPq for her MSc, PhD and PDJ scholarships.

References

Albuquerque, A.L., Meyers, P., Belem, A.L., Turcq, B., Siffedine, A., Mendoza, U., Capilla, R., 2016. Mineral and elemental indicators of post-glacial changes in sediment delivery and deposition under a western boundary upwelling system (Cabo Frio, southeastern Brazil). Palaeogeogr. Palaeoclimatol. Palaeoecol. 445, 72–82. http://dx.doi.org/10.1016/j.palaeo.2016.01.006.

Anjos, R.M., Veiga, R., Carvalho, C., Macario, K.D., Gomes, P.R.S., 2007. Geological provenance of Quaternary deposits from the southeastern Brazilian coast. Nucl. Phys. A 787, 642–647. http://dx.doi.org/10.1016/j.nuclphysa.2006.12.075.

Belem, A.L., Castelao, R.M., Albuquerque, A.L., 2013. Controls of subsurface temperature variability in a western boundary upwelling system. Geophys. Res. Lett. 40, 1362–1366. http://dx.doi.org/10.1002/grl.50297.

Berner, R.A., 1984. Sedimentary pyrite formation: an update. Geochim. Cosmochim. Acta 48, 605–615. http://dx.doi.org/10.1016/0016-7037(84)90089-9.

Blott, S.J., Pye, K., 2001. GRADISTAT: a grain size distribution and statistics package for the analysis of unconsolidated sediments. Earth Surf. Process. Landforms 26, 1237–1248. http://dx.doi.org/10.1002/esp.261.

Bucciarelli, E., Blain, S., Tréguer, P., 2001. Iron and manganese in the wake of the Kerguelen Islands (Southern Ocean). Mar. Chem. 73, 21–36. http://dx.doi.org/10.1016/S0304-4203(00)00070-0.

Busch, W.H., Keller, G.H., 1981. The physical properties of Peru-Chile continental margin sediments-the influence of coastal upwelling on sediment. J. Sediment. Petrol. 51, 705–719.

Calado, L., da Silveira, I.C.A., Gangopadhyay, A., de Castro, B.M., 2010. Eddy-induced upwelling off Cape São Tomé (22°S, Brazil). Cont. Shelf Res. 30, 1181–1188. http://dx.doi.org/10.1016/j.csr.2010.03.007.

Calado, L., Gangopadhyay, A., da Silveira, I.C.A., 2008. Feature-oriented regional modeling and simulations (FORMS) for the western South Atlantic: Southeastern Brazil region. Ocean Model. 25, 48–64. http://dx.doi.org/10.1016/j.ocemod.2008.06.007.

Campos, E.J.D., Velhote, D., da Silveira, I.C.A., 2000. Shelf break upwelling driven by Brazil Current Cyclonic Meanders. Geophys. Res. Lett. 27, 751–754. http://dx.doi.org/10.1029/1999GL010502.

Canfield, D.E., 1989. Reactive iron in marine sediments. Geochim. Cosmochim. Acta 53, 619–632. http://dx.doi.org/10.1016/0016-7037(89)90005-7.

Chan, L.S., Yeung, C.H., Yim, W.W.-S., Or, O.L., 1998. Correlation between magnetic susceptibility and distribution of heavy metals in contaminated sea-floor sediments of Hong Kong Harbour. Environ. Geol. 36, 77–86. http://dx.doi.org/10.1007/s002540050322.

Chen, S.-Y., Ambe, S., Takematsu, N., Ambe, F., 1996. The chemical states of iron in marine sediments by means of Mössbauer spectroscopy in combination with chemical leachings. J. Oceanogr. 52, 705–715.

Chorley, R.J., Schumm, S.A., Sugden, D.E., 1985. Geomorphology. Methuen & Co., New York.

Coelho-Souza, S.A., López, M.S., Guimarães, J.R.D., Coutinho, R., Candella, R.N., 2012. Biophysical interactions in the Cabo Frio upwelling system, southeastern Brazil. Braz. J. Oceanogr. 60, 353–365. http://dx.doi.org/10.1590/S1679-87592012000300008.

Cox, E.P., 1927. A method of assigning numerical and percentage values to the degree of roundness of sand grains. SEPM Soc. Sediment. Geol. 1, 179–183. http://dx.doi.org/10.2110/palo.2006.p06-106.

Cruz, A.P.S., Barbosa, C.F., Ayres-Neto, A., Albuquerque, A.L.S., 2013. Physical and geochemical properties of centennial marine sediments of the continental shelf of southeast Brazil. Geochim. Bras. 27, 1–12. http://dx.doi.org/10.5327/Z0102-9800201300010001.

de Oliveira, E.N., Knoppers, B.A., Lorenzzetti, J.A., Medeiros, P.R.P., Carneiro, M.E., de Souza, W.F.L., 2012. A satellite view of riverine turbidity plumes on the NE-E Brazilian coastal zone. Braz. J. Oceanogr. 60, 283–298. http://dx.doi.org/10.1590/S1679-87592012000300002.

Diaz, R., Moreira, M., Mendoza, U., Machado, W., Bottcher, M.E., Santos, H., Belem, A., Capilla, R., Escher, P., Albuquerque, A.L., 2012. Early diagenesis of sulfur in a tropical upwelling system, Cabo Frio, southeastern Brazil. Geology 40, 879–882. http://dx.doi.org/10.1130/G33111.1.

Drodt, M., Trautwein, A.X., König, I., Suess, E., Koch, C.B., 1997. Mössbauer spectroscopic studies on the iron forms of deep-sea sediments. Phys. Chem. Miner. 24, 281–293. http://dx.doi.org/10.1007/s002690050040.

Evans, M., Heller, F., 2001. Magnetism of loess/palaeosol sequences: recent developments. Earth-Sci. Rev. 54, 129–144. http://dx.doi.org/10.1016/S0012-8252(01)00044-7.

Fagel, N., 2007. Chapter four clay minerals, deep circulation and climate. Dev. Mar. Geol. 1, 139–184. http://dx.doi.org/10.1016/S1572-5480(07)01009-3.

Folk, R.L., Ward, W.C., 1957. Brazos River bar: a study in the significance of grain size parameters. J. Sediment. Petrol. 27, 3–26.
Frederichs, T., Bleil, U., Däumler, K., Dobeneck, T., Schmidt, A.M., 1999. The Magnetic View on the Marine Paleoenvironment: parameters, Techniques and Potentials of Rock Magnetic Studies as a Key to Paleoclimatic and Paleoceanographic Changes. In: Fischer, G., Wefer, G. (Eds.), Use of Proxies in Paleoceanography SE 24. Springer Berlin Heidelberg, pp. 575–599. http://dx.doi.org/10.1007/978-3-642-58646-0_24.
Gyllencreutz, R., Mahiques, M.M., Alves, D.V.P., Wainer, I.K.C., 2010. Mid- to late-Holocene paleoceanographic changes on the southeastern Brazilian shelf based on grain size records. Holocene 20, 863–875. http://dx.doi.org/10.1177/0959683610365936.
Hawthorne, F.C., 1988. Mossbauer Spectroscopy. In: Hawthorne, F.C. (Ed.), Spectroscopic Methods in Mineralogy and Geology. Mineralogical Society of America, Washington, pp. 255–340.
Karlin, R., Levi, S., 1983. Diagenesis of magnetic minerals in Recent haemipelagic sediments. Nature 303, 327–330. http://dx.doi.org/10.1038/303327a0.
Knoppers, B.A., Moreira, P.F., 1990. Material em suspensão e sucessão fitoplanctônica na lagoa de Guarapina - RJ. Acta Limnol. Bras.
Mahiques, M.M., Da Silveira, I.C.A., De Mello e Sousa, S.H., Rodrigues, M., 2002. Post-LGM sedimentation on the outer shelf-upper slope of the northernmost part of the São Paulo Bight, southeastern Brazil. Mar. Geol. 181, 387–400. http://dx.doi.org/10.1016/S0025-3227(01)00225-0.
Mahiques, M.M., Fukumoto, M.M., Silveira, I.C.A., Figueira, R.C.L., Bícego, M.C., Lourenço, R.A., Mello-e-Sousa, S.H., 2007. Sedimentary changes on the Southeastern Brazilian upper slope during the last 35,000 years. An. Acad. Bras. Cienc. 79, 171–181. http://dx.doi.org/10.1590/S0001-37652007000100018.
Mahiques, M.M., Mello e Sousa, S.H., Furtado, V.V., Tessler, M.G., Toledo, F.A. de L., Burone, L., Figueira, R.C.L., Klein, D.A., Martins, C.C., Alves, D.P.V., 2010. The southern Brazilian shelf: general characteristics, quaternary evolution and sediment distribution. Braz. J. Oceanogr. 58, 25–34.
Mahiques, M.M., Tessler, M.G., Maria Ciotti, A., Da Silveira, I.C.A., E Sousa, S.H.D.M., Figueira, R.C.L., Tassinari, C.C.G., Furtado, V.V., Passos, R.F., 2004. Hydrodynamically driven patterns of recent sedimentation in the shelf and upper slope off Southeast Brazil. Cont. Shelf Res. 24, 1685–1697. http://dx.doi.org/10.1016/j.csr.2004.05.013.
Mascarenhas, A.S., Miranda, L.B., Rock, N.J., 1971. A study of the oceanographic conditions in the region off Cabo Frio. In: Costlow Jr.J.D. (Ed.), Fertility of the Sea. Gordon & Breach, New York, pp. 31–44.
Matano, R.P., Palma, E.D., Piola, A.R., 2010. The influence of the Brazil and Malvinas currents on the southwestern Atlantic shelf circulation. Ocean Sci. Discuss. 7, 837–871. http://dx.doi.org/10.5194/osd-7-837-2010.
Mendoza, U., Neto, A.A., Abuchacra, R.C., Barbosa, C.F., Figueiredo, A.G.F., Gomes, M.C., Belem, A.L., Capilla, R., Albuquerque, A.L.S., 2014. Geoacoustic character, sedimentology and chronology of a cross-shelf Holocene sediment deposit off Cabo Frio, Brazil (southwest Atlantic Ocean). Geo-Mar. Lett. 34, 297–314. http://dx.doi.org/10.1007/s00367-014-0370-6.
Minai, Y., Makamura, Y., Tominaga, T.A., 1981. Mössbauer study of oceanic sediments from site 612. In: Turner, K.L. (Ed.), Initial Reports of the Deep Sea Drilling Project, Leg 95. Deep Sea Drilling Project, Washington, pp. 641–645.
Moore, W.S., 1984. Radium isotope measurements using germanium detectors. Nucl. Instrum. Methods Phys. Res. 223, 407–411. http://dx.doi.org/10.1016/0167-5087(84)90683-5.
Morton, A.C., Hallsworth, C.R., 1999. Processes controlling the composition of heavy mineral assemblages in sandstones. Sediment. Geol. 124, 3–29. http://dx.doi.org/10.1016/S0037-0738(98)00118-3.
Muehe, D., Carvalho, V.G. De, 1993. Geomortologla, cobertura sedimentar e transporte de sedimentos na plataforma continental interna entre a Ponta de Saquarema e o Cabo Frio (RJ). Bol. do Inst. Ocean. 41, 1–12.
Nobrega, J.E.S., Sawakuch, A.O., Almeida, R.P. De, 2008. Minerais pesados das porções média e superior do Grupo Guaritas (Eocambriano, RS): considerações sobre a proveniência sedimentar. Rev. Bras. Geociênc. 38, 554–565.
Passier, H.F., Dekkers, M.J., de Lange, G.J., 1998. Sediment chemistry and magnetic properties in an anomalously reducing core from the eastern Mediterranean Sea. Chem. Geol. 152, 287–306. http://dx.doi.org/10.1016/S0009-2541(98)00121-1.
Pattan, J.N., Parthiban, G., Banakar, V.K., Tomer, A., Kulkarni, M., 2008. Relationship between chemical composition and magnetic susceptibility in sediment cores from Central Indian Ocean Basin. J. Earth Syst. Sci. 117, 113–119. http://dx.doi.org/10.1007/s12040-008-0002-5.
Powers, M.C., 1953. A new roundness scale for sedimentary particles. J. Sediment. Petrol. 23, 117–119. http://dx.doi.org/10.1306/d4269567-2b26-11d7-8648000102c1865d.
Remus, M.V.D., Souza, R.S., Cupertino, J.A., De Ros, L.F., Dani, N., Vignol-Lelarge, M.L., Vinicius, M., Remus, D., Vinicius, M., Remus, D., Souza, R.S., Cupertino, J.A., Ros, L.F., De, Dani, N., Vignol-Lelarge, M.L., 2008. Proveniência sedimentar: métodos e técnicas analíticas aplicadas. Rev. Bras. Geociênc. 38, 166–185. http://dx.doi.org/10.5327/Z1519-874×201300040003.
Rocha, J., Milliman, J.D., Santana, C.I., Vicalvi, M.A., 1975. Southern Brazil. upper continental margin sedimentation off Brazil. Contrib. Sedimentol. 4, 117–150.
Rodrigues, R.R., Rothstein, L.M., Wimbush, M., 2007. Seasonal Variability of the South Equatorial Current Bifurcation in the Atlantic Ocean: a Numerical Study. J. Phys. Oceanogr. 37, 16–30. http://dx.doi.org/10.1175/JPO2983.1.
Rossetti, D.F., Bezerra, F.H.R., Góes, A.M., Neves, B.B.B., 2011. Sediment deformation in Miocene and post-Miocene strata, northeastern Brazil: Evidence for paleoseismicity in a passive margin. Sediment. Geol. 235, 172–187. http://dx.doi.org/10.1016/j.sedgeo.2010.02.005.
Sanders, C.J., Caldeira, P.P., Smoak, J.M., Ketterer, M.E., Belem, A., Mendoza, U.M.N., Cordeiro, L.G.M.S., Silva-Filho, E.V., Patchineelam, S.R., Albuquerque, A.L.S., 2014. Recent organic carbon accumulation (~100 years) along the Cabo Frio, Brazil upwelling region. Cont. Shelf Res. 75, 68–75. http://dx.doi.org/10.1016/j.csr.2013.10.009.
Schultheiss, P.J., Weaver, P.P.E., 1992. Multi-sensor Core Logging For Science And Industry, In: OCEANS 92 Mastering the Oceans Through Technology. Proceedings. IEEE, pp. 608–613. doi:10.1109/OCEANS.1992.607652.
Schulz, H.D., Schulz, H.D., 1999. Marine Geochemistry. doi:10.1 007/978-94-010-9488-7 e-ISBN-13:978-94-0.
Scorzelli, R.B., Bertolino, L.C., Luz, A.B., Duttine, M., Silva, F.A.N.G., Munayco, P., 2008. Spectroscopic studies of kaolin from different Brazilian regions. Clay Miner. 43, 129–135. http://dx.doi.org/10.1180/claymin.2008.043.1.10.
Seeberg-Elverfeldt, J., Schlüter, M., Feseker, T., Kölling, M., 2005. Rhizon sampling of pore waters near the sediment/water interface of aquatic systems. Limnol. Oceanogr. Methods 3, 361–371. http://dx.doi.org/10.4319/lom.2005.3.361.
Silveira, I.C.A., Lima, J.A.M., Schmidt, A.C.K., Ceccopieri, W., Sartori, A., Franscisco, C.P.F., Fontes, R.F.C., 2008. Is the meander growth in the Brazil current system off Southeast Brazil due to baroclinic instability? Dyn. Atmos. Ocean. 45, 187–207. http://dx.doi.org/10.1016/j.dynatmoce.2008.01.002.
Stucki, J.W., Low, P.F., Roth, C.B., Golden, D.C., 1984. Effects of oxidation state of octahedral iron on clay swelling. Clays Clay Miner. 32, 357–362.
Suguio, K., 1980. Rochas Sedimentares: propriedades, Gênese e Importância Econômica. Edgard Blücher Ltda./EDUSP, São Paulo.
Valentin, J.L., 2001. The Cabo Frio Upwelling System, Brazil. In: Seeliger, U., Kjerfve, B. (Eds.), Coastal Marine Ecosystems of Latin America. Springer Berlin Heidelberg, Berlin, Heidelberg, pp. 97–105. http://dx.doi.org/10.1007/978-3-662-04482-7_8.
van Santvoort, P.J.M., de Lange, G.J., Langereis, C.G., Dekkers, M.J., Paterne, M., 1997. Geochemical and paleomagnetic evidence for the occurrence of "missing" sapropels in eastern Mediterranean sediments. Paleoceanography 12, 773–786. http://dx.doi.org/10.1029/97PA01351.
Viana, A.R., Faugeres, J.C., Kowsmann, R.O., Lima, J.A.M., Caddah, L.F.G., Rizzo, J.G., 1998. Hydrology, morphology and sedimentology of the Campos continental margin, offshore Brazil. Sediment. Geol. 115, 133–157. http://dx.doi.org/10.1016/S0037-0738(97)00090-0.
Villasante-Marcos, V., Hollis, C.J., Dickens, G.R., Nicolo, M.J., 2009. Rock magnetic properties across the Paleocene-Eocene thermal maximum in Marlborough, New Zealand. Geol. Acta 7, 229–242.
Wanderley, C.V.A., Godoy, J.M., Godoy, M.L.D.P., Rezende, C.E., Lacerda, L.D., Moreira, I., Carvalho, Z.L., 2013. Evaluating Sedimentation Rates in the Estuary and Shelf Region of the Paraíba do Sul River, Southeastern Brazil. J. Braz. Chem. Soc. 50–64. http://dx.doi.org/10.5935/0103-5053.20130268.
Yamazaki, T., Solheid, P.A., Frost, G.M., 2000. Rock magnetism of sediments in the Angola-Namibia upwelling system with special reference to loss of magnetization after core recovery. Earth Planets Sp. 52, 329–336. http://dx.doi.org/10.2312/cr_msm20_3.